SYNTHESIS, CHARACTERIZATION, AND GAS-SENSING PROPERTIES OF α-Fe$_2$O$_3$ PREPARED FROM Fe$_3$O$_4$-ALGINATE

Nguyen Duc Cuong[1,2*]**, Tran Thai Hoa**[1]**, Dinh Quang Khieu**[1]**, Truong Quy Tung**[1]**, Nguyen Van Hieu**[3]

[1]*College of Sciences, Hue University*

[2]*Faculty of Hospitality and Tourism, Hue University*

[3]*International Training Institute for Materials Science, Hanoi University of Science Technology*

Abstract

In this study, nanocomposite Fe$_3$O$_4$–alginate has been prepared by so-called two step method. The crystal structures and morphologies of as-synthesized nanopaticles (NPs) were characterized X-ray diffraction, and scanning electron microscopy. The surface states of Fe$_3$O$_4$-alginate NPs were characterized by Fourier transform infrared spectra. α-Fe$_2$O$_3$ was fabricated from the nanocomposite Fe$_3$O$_4$-alginate by heat treatment in air atmosphere at 600 °C and their gas sensing properties were investigated. The performance of the α-Fe$_2$O$_3$ in the detection of toxic and flammable gases such as carbon oxide, ammonia, liquefied petroleum gas, ethanol, and hydrogen was evaluated. The Fe$_2$O$_3$ based gas sensors exhibited high sensitivity and a response time of less than a minute to analytic gases.

Keywords: Fe$_2$O$_3$, Fe$_3$O$_4$, gas sensor, alginate.

1. INTRODUCTION

Iron oxyhydroxides and iron oxides are such abundant materials. Goethite (α-FeOOH) can be used as electrode materials, and is the most important precursor of hematite. Hematite (α-Fe$_2$O$_3$) is the most stable iron oxide under ambient conditon with low cost, environmental friendliness, and fascinating physicochemical properties, which has been widely used in diverse fields contain catalysis, chemical sensor, magnetic devices, and electrode materials [1]. Stimulated by these intriguing propertises and potential applications, a wide variety of iron oxide nano-structures, such as NPs [2], nanorods [3], nanocubics [4] and nanoleaves [5] have been synthesized through various methods.

Aside from ferric oxide, magnetite (Fe$_3$O$_4$), an important kind of magnetic material with a cubic inverse spinal structure, has also been received increasing attention because of its wide use in magnetic recording, ferrofluid, catalyst, magnetic resonance imaging (MRI), bio-separation, drug targeting, and hyperthermia [6]. To improve the colloidal stability of NPs, the surface of NPs could be modified with a polymer [7]. Among these materials, alginate is the major structural polysaccharide of marine brown algae, and it has combined features of abundant resources, low-cost, and biocompatible. Thus, alginate is a suitable polymer for the modificatin of Fe$_3$O$_4$ NPs.

In the present study, we intorduced the synthesis of Fe$_3$O$_4$ NPs through a co-precipitation process and subsequently modified the synthesized NPs with alginate. The adsorption and modification of alginate onto the surface of Fe$_3$O$_4$ NPs were investigated to optimize the colloidal stability of Fe$_3$O$_4$ NPs. Strucrure of synthesized NPs were investigated using advanced techniques. Furthermore, Fe$_3$O$_4$-alginate were transformed into α-Fe$_2$O$_3$ phase by heat treatment in air atmosphere at high temperature for gas sensing applications.

2. EXPERIMENTAL

2.1. Materials

All reagents were analytical grade and used as received without further purification. Ferric chloride hexahydrate (FeCl$_3$.6H$_2$O, Merck), ferrous chloride tetrahydrate (FeCl$_2$.4H$_2$O, Merck), and alginate (Quangzi, China) were used as iron and polymer stabilizer sources, respectively. NaOH (Quangzi, China were used to adjust the pH of solutions for co-precipitation of Fe$_3$O$_4$ NPs.

2.2. Preparation of Fe₃O₄ particles and Fe₃O₄-chitosan

Fe_3O_4 NPs were synthesized through the coprecipitation method using ferric and ferrous chloride as iron sources. In a typical synthesis, ferric chlorides (2 mmol) and ferrous chlorides (1 mmol) were dissolved in 100 mL H_2O to obtain a homogemous solution. Chemical precipitation was achieved by slow adding 0,1 mol.L^{-1} NaOH solution at 80 °C with stirred vigorously for 30 min. The products were recovered by filtering, washing, drying at 60 °C. Then Fe_3O_4 powder was dispersed in distilled water (1 g/100 mL), the Fe_3O_4 suspension was added slowly alginate solution (2 g/100 mL) with vigorous stirring at 50 °C for 30 minutes. The modified Fe_3O_4-alginate NPs were recovered through filtering, washing, and drying at room temperature.

X-ray diffraction (XRD) was performed to identify the structure of Fe_3O_4, Fe_3O_4-alginate, and Fe_2O_3 (D8 Advance, Brucker, Germany). Morphologies were studied by scanning electron microscopy (SEM, Model JSM-5300LV). Infrared (IR) spectra were recorded with Nicolet 6700 FTIR Spectrometer.

2.3. Sensor fabrication and gas-sensing tests

To characterize the gas sensing properties, synthesized Fe_3O_4-alginate NPs were dispersed in ethanol and deposited on a pre-fabricated interdigitated electrode substrate using a micropipette. Fe_3O_4-alginate films were then treated with heat in normal atmospheric conditons at 600 °C for 5h to transform Fe_3O_4 into the α-Fe_2O_3 phase.

The gas sensing properties of α-Fe_2O_3 NPs were studied by testing sensor with H_2 (25-500 ppm), CO (10-100 ppm), C_2H_5OH (50-500 ppm), and NH_3 (50–5000 ppm) at different temperatures (300–400 °C) using a homemade set up with high speed switching gas flow (from/to air to/from balance gas). Balance gases (0.1% in air) were purchased from Air Liquid Group (Singapore). Flow through of the system was employed with a constant flow-rate of 200sccm. Detail information about the gas testing system is presented in [8].

3. RESULTS AND DISCUSSION

The crystal structure and phase transformation of Fe_3O_4-alginate and Fe_2O_3 NPs revealed by XRD are presented in Fig. 1a and b. XRD patterns of Fe_3O_4-

alginate exhibited typical Fe_3O_4 cubic structure, where all diffraction peaks well indexed to the (220), (311), (400), (422), (511), and (440) planes (JCPDS No. 19-0629). However, after calcination at 600 °C for 5h (Fig. 1b), the cubic Fe_3O_4 was converted into α-Fe_2O_3. The main peaks of α-Fe_2O_3 are indexed to a rhombohedral profile characteristics of the α-Fe_2O_3 crystal structure (JCPDS No. 81e2810). No detectable peak of impurities and other phases was observed, indicating the formation of single-phase α-Fe_2O_3. The average crystalline sizes of the Fe_3O_4-alginate and α-Fe_2O_3 NPs calculated from the XRD data using the Scherrer equation ($d = 0.9\lambda/(\beta cos\theta)$) are about 15 and 20 nm, respectively.
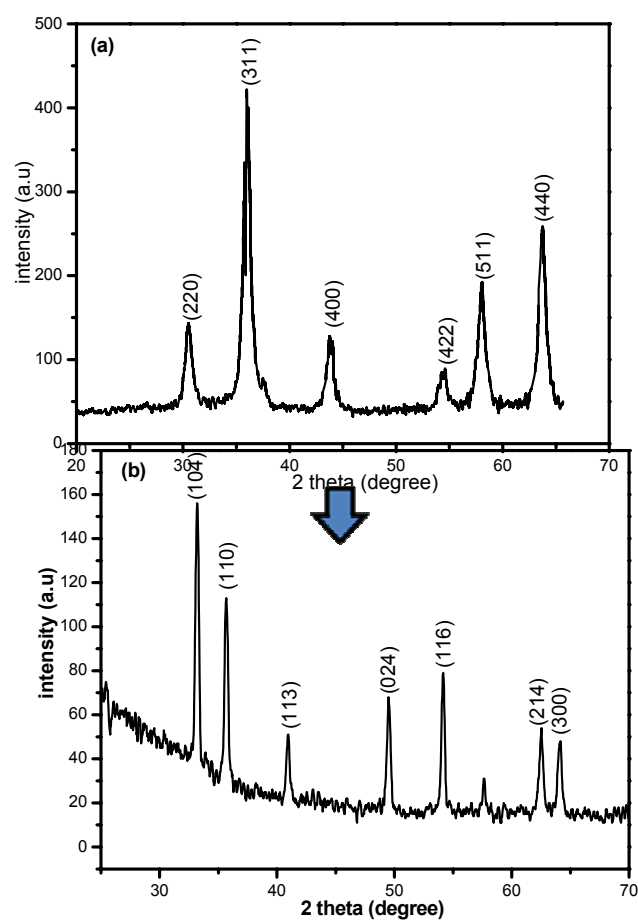

Figure 1: XRD pattern of Fe_3O_4-alginate (a) and Fe_2O_3 obtained from heat treatment of Fe_3O_4-alginate (b)

The morphologies of the Fe_3O_4-alginate and α-Fe_2O_3 obtained from heatment of Fe_3O_4-alginate were characterized by SEM (Fig. 2). SEM micrographs of Fe_3O_4-alginate (Fig. 2a) demonstrate that their diameters were in the range of 10–15 nm. These results are consistent with those obtained by

size calculation from XRD. The α-Fe$_2$O$_3$ NPs are irregularly shaped and they are aggregated because of the grain growth that occurred at a high calcination temperature. The average particle size of α-Fe$_2$O$_3$, as observed from the micrograph, was of the order of 150 nm. This result indicates that the α-Fe$_2$O$_3$ NPs are not single crystals but are polycrystalline in nature.
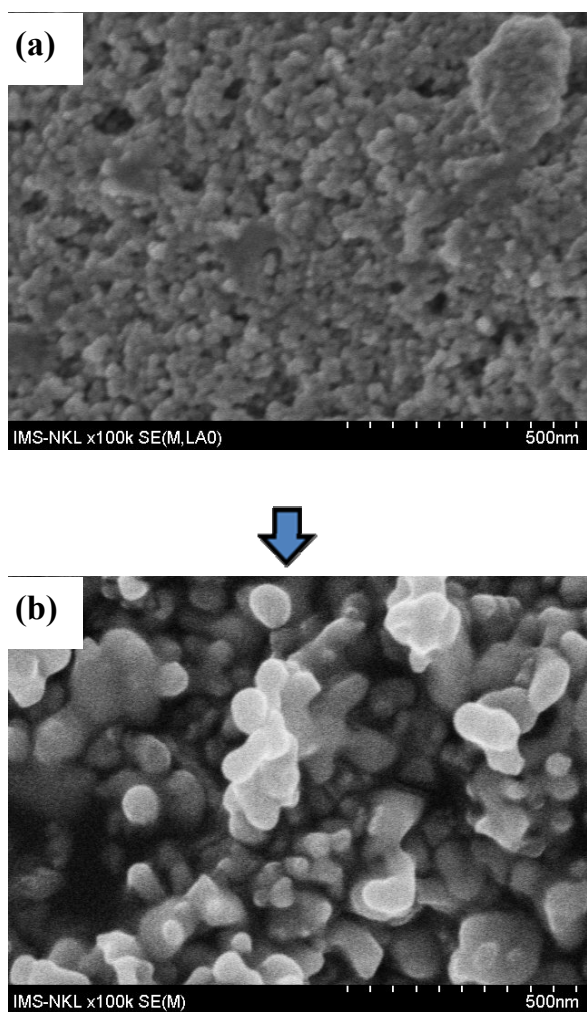

Fig. 2: SEM of Fe$_3$O$_4$-alginate (a) and and Fe$_2$O$_3$ obtained from heat treatment of Fe$_3$O$_4$-alginate (b)

The binding of Fe$_3$O$_4$ to alginate was also confirmed by FT-IR analysis. Fig. 3 shows the FT-IR of spectra of alginate (a), pristine Fe$_3$O$_4$ NPs (b) and Fe$_3$O$_4$-alginate (c). The characteristic peaks of Fe$_3$O$_4$ at 580 and 560 cm^{-1} could be observed in both of (b) and (c) which indicated that the nanoparticles were Fe$_3$O$_4$. As for the alginate spectrum, the carboxyl group of alginate has a single-band character of $\nu_{as}(COO^-)$ and $\nu_s(COO^-)$, and the values are 1622 cm^{-1} and 1420 cm^{-1}, respectively. In the spectrum of alginate, $\nu_{as}(COO^-)$ and $\nu_s(COO^-)$ were changed to frequencies of 1615 cm^{-1} and 1400 cm^{-1}, and ν(Fe-O) to a lower frequency of 560 cm^{-1}, suggesting that Fe$_3$O$_4$ was bound to alginate. This can be interpreted by assuming that COO$^-$ terminal of alginate coordinates to Fe of Fe$_3$O$_4$ by complex formation. As a result, Fe$_3$O$_4$ NPs were bound with alginate and this interaction might be as strong as a hydrogen bond, which also explains the high stability of alginate-Fe$_3$O$_4$. The capping of aginate around Fe$_3$O$_4$ confirmed by FT-IR, the interaction being via bridging oxygen of carboxylate and the nanoparticle surface was reported by several papers [7, 9].

We systematically investigated the gas-sensing performance of Fe$_2$O$_3$ sensors prepared from heat-treatment of Fe$_3$O$_4$-alginate, hereafter referred to as "Fe$_2$O$_3$-A sensor". Sensor was tested with various gases (H$_2$, CO, C$_2$H$_5$OH, and NH$_3$) at different gas concentrations and working temperatures.

Fig. 4a and b presents the H$_2$ sensing characteristics of Fe$_2$O$_3$-A sensors. The typical responses of these sensors to 500 ppm H$_2$ at 300, 350, and 400 $^{\circ}$C demonstrate that the optimum operating temperature for sensor is 350 $^{\circ}$C. The response of the sensor to various concentrations at optimum operating temperature of H$_2$ gas (Fig. 4b) demonstrated that the response of the Fe$_2$O$_3$-A sensor is significant enhanced with H$_2$ gas concentration. H$_2$ sensors have been extensively investigated [10], although studies on H$_2$ sensors based on Fe$_2$O$_3$ are few. The Fe$_2$O$_3$-A sensor were also tested with CO gas applying the same procedure used for H$_2$ gas testing (Fig. 4c and d). Responses of the sensor slightly varied at the operating temperature range of 300-400 $^{\circ}$C. The optimum operating temperature was 350 $^{\circ}$C, which concurs with the results of the H$_2$ gas test.

The ethanol sensing characteristics of Fe$_2$O$_3$-A sensor was also investigated. Fig. 4e and f shows the transient response of the sensor to 500 ppm C$_2$H$_5$OH at different operating temperatures (300, 350, and 450 $^{\circ}$C). The optimum operating temperature of the Fe$_2$O$_3$-A sensor is 350 $^{\circ}$C. The NH$_3$ gas detection ability of α-Fe$_2$O$_3$-based sensors has not been fully explored [11, 12]. The transient responses of α-Fe$_2$O$_3$-A sensor to 500 ppm NH$_3$ at different operating temperatures (300, 350, and 400 $^{\circ}$C) are shown in Fig. 4g and h. The sensor has an optimum operating temperature of 300 $^{\circ}$C, which was lower than that found in the H$_2$, CO, and ethanol tests.
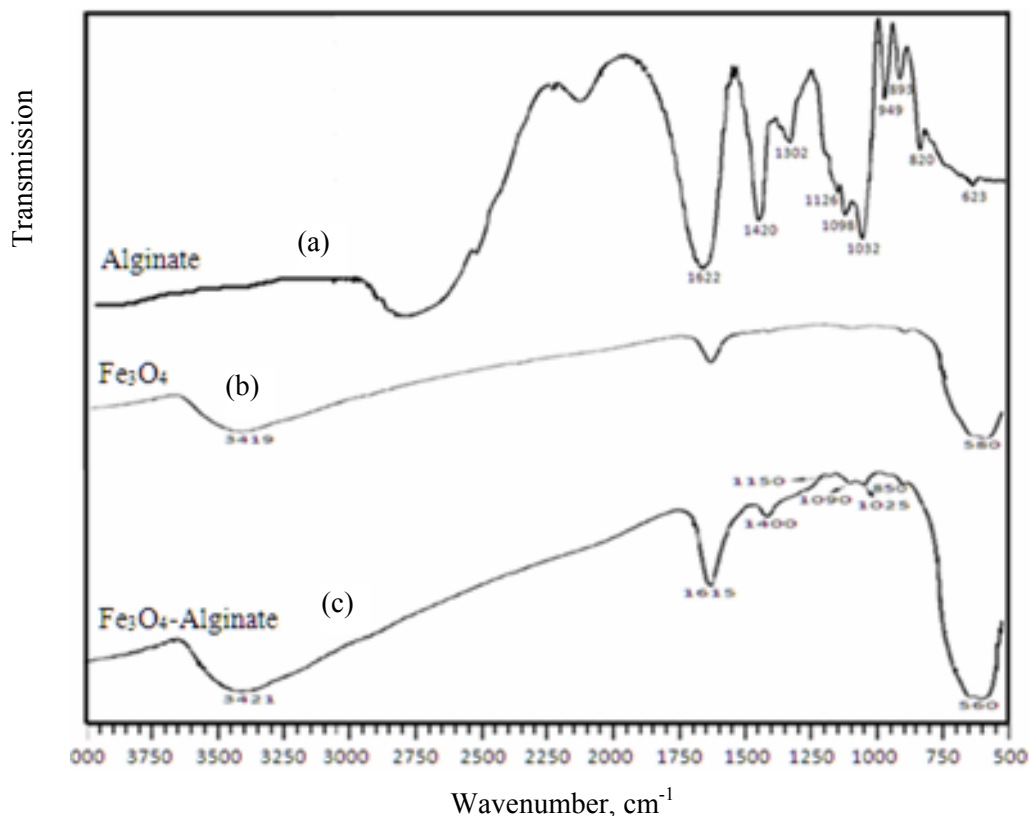
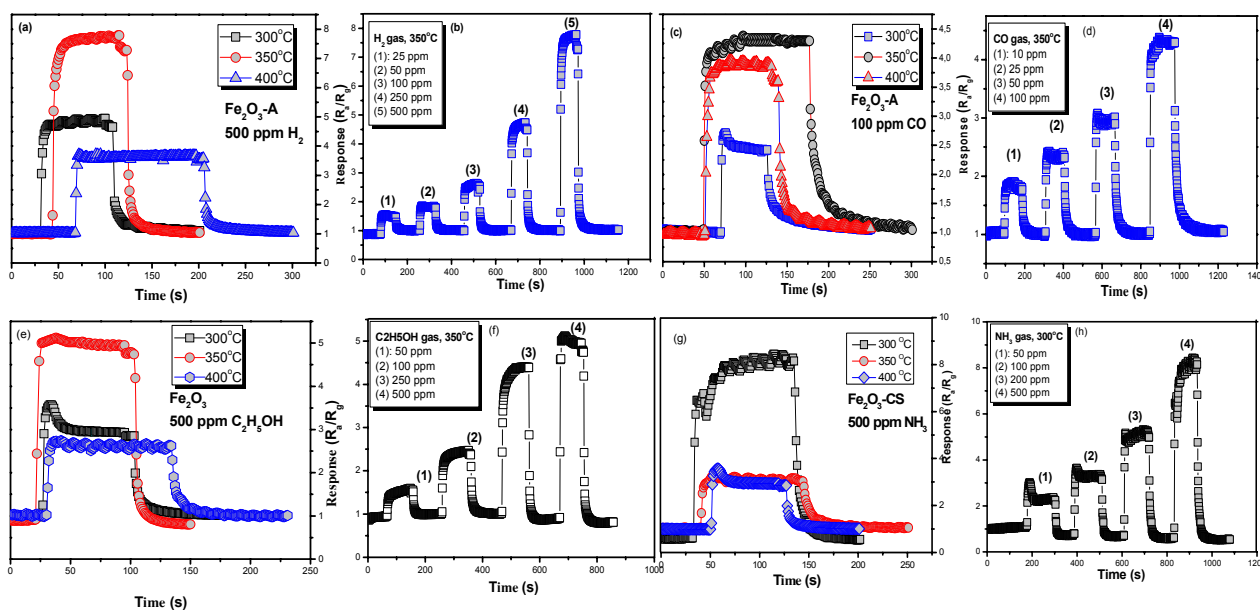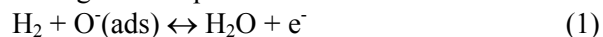*Figure 3:* FT-IR of spectra of alginate (a), pristine Fe_3O_4 NPs (b), Fe_3O_4-alginate (c)

Figure 4: The response of α-Fe_2O_3-A sensor for H_2 (a, b), CO (c, d), C_2H_5OH (e, f), and NH_3 (g, h) gases at different operating temperatures and various concentration

The sensing mechanism of the Fe_2O_3 NP-based gas sensors to these reducing gases can be explained by the depletion region. During the gas-sensing measurement, the oxygen in the air captured the electrons from the Fe_2O_3 crystal and ion-adsorbed (O^{-2}, O^- and O^{2-}) on the surface of the sensing layer;

this phenomenon resulted in the formation of the electron-depletion region [13]. Upon exposure to H_2, CO, C_2H_5OH, and NH_3, these molecules interacted with the pre-adsorbed oxygen and released electrons, according to the equations:

$$H_2 + O^-(ads) \leftrightarrow H_2O + e^- \tag{1}$$

$$CO + O^-(ads) \leftrightarrow CO_2 + e^- \qquad (2)$$

$$C_2H_5OH + 6O^-(ads) \leftrightarrow 2CO_2 + 3H_2O + 6e^- \qquad (3)$$

$$2NH_3 + 7O^-(ads) \leftrightarrow 2NO_2 + 3H_2O + 7e^- \qquad (4)$$

$$C_nH_{2n+1} + 2O^- \leftrightarrow H_2O + C_nH_{2n}O^- + e^- \qquad (5)$$
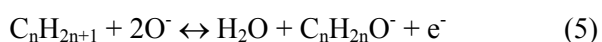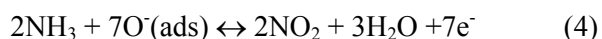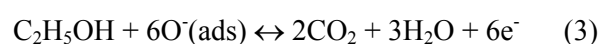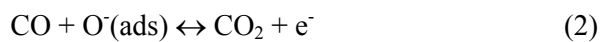
4. CONCLUSION

In this study, The Fe_3O_4–alginate NPs with core-shell structure core were susscessfully prepared by coprecipitation method. The particle size of the composite NPs was 10-15 nm. The interaction of Fe_3O_4 NPs and alginate were confirmed using IR. The performance of α-Fe_2O_3 sensor obtained from alginate-coated Fe_3O_4 were tested at different operating temperatures and tovarious gases (e.g. H_2, CO, C_2H_5OH, and NH_3). The α-Fe_2O_3 sensor prepared from alginate-coated Fe_3O_4 NPs showed good performance. In comparison with all tested gases, the α-Fe_2O_3 based sensors exhibited relatively good response to H_2 gas.

REFERENCES

1. Q. Hao, S. Liu, X. Yin, Y. Wang, Q. Li, T. Wang. *Facile synthesis of 3D flowerlike a-FeOOH architectures and their conversion into mesoporous α-Fe₂O₃ for gas-sensing application*, Solid State Sci., **12**, 2125-2129 (2010).

2. N. D. Cuong, T. T. Hoa, D. Q. Khieu, N. D. Hoa, N. V. Hieu. *Gas sensor based on nanoporous hematite nanoparticles: Effect of synthesis pathways on morphology and gas sensing properties*, Curr. Appl. Phys., **12**, 1355-1360 (2012).

3. H. K. Mulmudi, N. Mathews, X. C. Dou, L. F. Xi, S. S. Pramana, Y. M. Lam, S. G. Mhaisalkar. *Controlled growth of hematite (α-Fe₂O₃) nanorod array on fluorine doped tin oxide: Synthesis and photoelectrochemical properties*, Electrochem.

Commun., **13**, 951-954 (2011).

4. Y. Wang, H. Yang. *Synthesis of iron oxide nanorods and nanocubes in an imidazolium ionic liquid*, Chem. Eng. J., **147**, 71-78 (2009).

5. Y. Y. Xu, D. Zhao, X. J. Zhang, W. T. Jin, P. Kashkarov, H. Zhang. *Synthesis and characterization of single-crystalline α-Fe₂O₃ nanoleaves*, Physica E, **41**, 806-811 (2009).

6. Y. F. Shen, J. Tang, Z. H. Nie, Y. D. Wang, Y. Ren, L. Zuo. *Preparation and application of magnetic Fe₃O₄ nanoparticles for wastewater purification*, Sep. Purif. Technol., **68**, 312-319 (2009).

7. X. Q. Xu, H. Shen, J. R. Xu, M. Q. Xie, X. J. Li. *The colloidal stability and core-shell structure of magnetite nanoparticles coated with alginate*, Appl. Surf. Sci., **253**, 2158-2164 (2006).

8. L. V. Thong, L. T. N. Loan, N. V. Hieu, *Comparative study of gas sensor performance of SnO₂ nanowires and their hierarchical nanostructures*, Sensor Actuat. B-Chem., **150**, 112119 (2010).

9. Hui Li Ma, Yu Feng Xu, Xian Rong Qi, Yoshie Maitani, Tsuneji Nagai. *Superparamagnetic iron oxide nanoparticles stabilized by alginate: Pharmacokinetics, tissue distribution, and applications in detecting liver cancers*, Int. J. Pharm., **354**, 217-226 (2008).

10. T. Hübert, L. Boon-Brett, G. Black, U. Banach. *Hydrogen sensors - A review*, Sensor. Actuat. B-Chem., **157**, 329-352 (2011).

11. K. Hara, N. Nishida. *H₂ sensor using Fe₂O₃-based thim film*, Sensor. Actuat. B-Chem., **20**, 181-186 (1994).

12. D. R. Patil, L. A. Patil. *Preparation and study of NH₃ gas sensing behavior of Fe₂O₃ doped ZnO thick film resistors*, Sensors & Transducers, **70**, 661-670 (2006).

13. R. L. Vander Wal, G. W. Hunte, J. C. Xub, M. J. Kulis, G. M. Berger, T. M. Ticich. *Metal-oxide nanostructure and gas-sensing performance*, Sensor. Actuat. B-Chem., **138**, 113-119 (2009).

Corresponding author: **Nguyen Duc Cuong**
College of Sciences, Hue University
77 Nguyen Hue, Phu Nhuan Award, Hue City
Email: nguyenducna@gmail.com
Tel.: 0935.27.9996.